Talanta 178 (2018) 1046–1052

Contents lists available at ScienceDirect

Talanta

journal homepage: www.elsevier.com/locate/talanta

A regenerative and selective electrochemical aptasensor based on copper oxide nanoflowers-single walled carbon nanotubes nanocomposite for chlorpyrifos detection

Guoli Xu[a], Danqun Huo[a,*], Changjun Hou[a], Yanan Zhao[a], Jing Bao[a], Mei Yang[a], Huanbao Fa[b]

[a] Key Laboratory of Biorheology Science and Technology, Ministry of Education, College of Bioengineering, Chongqing University, Chongqing 400044, China
[b] College of Chemistry and Chemical Engineering, Chongqing University, Chongqing 400044, China

ARTICLE INFO

Keywords:
Aptamer
Single walled carbon nanotubes
Copper oxide nanoflowers
Chlorpyrifos
Regenerative

ABSTRACT

Chlorpyrifos is a commonly used organophosphorus pesticide in agriculture. However, its neurotoxicity poses a huge threat to human health. To detect trace amounts of chlorpyrifos, we herein developed a regenerative electrochemical aptasensor for the sensitive detection of chlorpyrifos. The nanocomposite consisting of copper oxide nanoflowers (CuO NFs) and carboxyl-functionalized single walled carbon nanotubes (c-SWCNTs) was prepared to improve the sensing performance for chlorpyrifos detection. Various characterization methods such as scanning electron microscopy (SEM), fourier transform infrared spectroscopy (FT-IR) and cyclic voltammetry (CV) were used to demonstrate the successful fabrication of biosensor. Differential pulse voltammetry (DPV) was utilized to optimize test conditions and quantify chlorpyrifos. Under optimal conditions, the biosensor obtained a good linearity for chlorpyrifos ranging from 0.1 to 150 ng/mL, with a lower detection limit of 70 pg/mL. This aptasensor also exhibited high selectivity and outstanding repeatability, and was successfully applied to the determination of chlorpyrifos in spiked apple and celery cabbage with satisfactory recoveries. Furthermore, the sensor can be easily regenerated by urea for continuous application. With all the features, the proposed strategy provides an excellent platform for regenerative and selective detection of chlorpyrifos.

1. Introduction

Organophosphorus pesticide (OP) is one of the most commonly used pesticides in the world, especially in developing countries [1] and can be converted into neurotoxic agents used in chemical weapons. Due to its inhibition of the activity of acetylcholinesterase (AChE) or cholinesterase (ChE) in the nervous system, OP can destroy the normal nerve impulse conduction, causing a series of poisoning symptoms, such as abnormal excitement, spasm, paralysis and death [2–5]. Thus, OP is attracting more and more countries to set stricter standards for OP's secure applications. Chlopyrifos (O,O-Diethyl-O-(3,5,6-trichloro-2-pyridyl) phosphorothioate), a Class II toxicant, is one of the most used broad-spectrum OPs over the past decade [6]. From the latest reports, chlorpyrifos is also associated with cancer [7], chronic obstructive pulmonary disease [8], asthma [9] and reproductive system injury [10]. The widespread use of OPs in soil and water has already resulted in serious contaminations of drinking water and soil, and brings the serious health threats to humans. Therefore, in order to control this toxic pesticide, it is highly desired to develop sensitive and specific methods for the detection of OPs.

Over the last two decades, numerous analytical methods have been carried out for the determination of OPs, such as HPLC [11], GC-MS [12], continuous flow system [13], infrared micro-imaging [14], photoelectrochemical sensing [15] and thin-layer chromatography [16]. Despite their high sensitivity and accuracy, these methods are not desirable for in-field application owing to the shortcomings, such as high cost, complex sample preparation, and high requirement of professional operation. On the other hand, antibody-based detection technology shows high sensitivity and specificity, but the implementation of antibodies still faces many limitations, such as easy inactivation, difficulty of being modified [17]. To overcome these problems, aptamer-based biosensor exhibits distinct advantages. Aptamer is a single-stranded DNA or RNA oligonucleotide molecule that is chemically synthesized in vitro and capable of binding target molecule with high specificity and affinity. Due to the diversity of random oligonucleotide libraries, theoretically, aptamer can be screened through the technique of systematic evolution of ligands by exponential enrichment (SELEX) against numerous targets, including heavy metal ions [18,19], small organic molecules [20], proteins [21] and viruses [22]. Compared with the antibody, aptamer has apparent advantages of easier preparation and

* Corresponding author.
E-mail address: huodq@cqu.edu.cn (D. Huo).

http://dx.doi.org/10.1016/j.talanta.2017.08.086
Received 15 May 2017; Received in revised form 21 August 2017; Accepted 27 August 2017
Available online 30 August 2017

preservation, more convenient modification, and higher thermal stability. Aptamers have been applied in the development of various biosensors via different detection strategies such as electrochemistry [18,20,21], fluorescence [19], colorimetry [23] and surface-enhanced Raman spectroscopy (SERS) [24]. Currently, the electrochemical method is a very attractive choice for trace analysis due to its high sensitivity, rapid response, and easy miniaturization. As is well known, many nanomaterials have been introduced into the study of sensors to enhance the sensing performance, such as noble metals [25], carbon materials [26], conducting polymers [27] and metal oxides [28]. Recently, Sun etc. reported an electrochemical aptasensor based on OMC-CS and Fc@WMCNTs-CS double-assisted signal amplification strategy for chlorpyrifos detection [29], Jiao etc. also reported developed a sensitive electrochemical aptasensor based on a nanostructure consisting of carbon black and graphene oxide@Fe3O4 for detection of chlorpyrifos [30], but the regeneration of chlorpyrifos aptasensor was not involved. The reusability of a single electrode is a very critical factor of an electrochemical biosensor in detecting real samples. Consequently, it is vital to explore the regeneration of aptasensor.

In this study, for the first time, we developed a regenerative and selective electrochemical aptasensor for chlorpyrifos detection based on copper oxide nanoflowers and single walled carbon nanotubes (CuO NFs-SWCNTs) nanocomposite. Here, we employed CuO NFs as a potential candidate to expand the surface area of the electrode because of its three-dimensional nanostructure with low cost and excellent chemical stability. Furthermore, carbon nanotubes (CNTs) have excellent mechanical properties, superior biocompatibility and electrical properties that can amplify sensing signal and increase electron transfer rate. Herein, c-SWCNTs were utilized to enhance the ability of immobilizing the aminated probes and hybridization between aptamers and aminated probes. For the study of the regeneration of aptasensor, urea was employed to remove semi-duplex from the sensing electrode and the aptasensor showed favorable stability after five regenerations. Moreover, under optimized conditions, the electrochemical measurement results show that the fabricated sensor exhibits excellent electrochemical performance with high selectivity, low detection limit and outstanding reproducibility. This biosensor was further successfully used for analysis of real samples, showing significant potential for broad applications in the field of food safety and public health security.

2. Materials and methods

2.1. Materials and reagents

Copper (II) sulfate pentahydrate ($CuSO_4{\cdot}5H_2O$), sodium hydroxide (NaOH), ethanol, sodium dodecyl sulfate (SDS) and urea were purchased from Chongqing Chuan-dong Chemical Group (China). Carboxylated single-walled carbon nanotubes (c-SWCNTs) were bought from Nanjing Xianfeng Nanomaterials Co. (China). Nafion 117 solution and N, N-dimethylformamide (DMF, anhydrous, 99.8%) were acquired from Sigma-Aldrich. 1-ethyl-3-(3-dimethylaminopropyl) carbodiimide (EDC), N-hydroxy-succinimide (NHS) and sodium dodecyl sulfate (SDS) were purchased from Aladdin Industrial Corporation (USA). Methylene blue (MB) was procured from Chengdu Kelong Chemical Reagent Factory. Chlopyrifos, fenitrothion, omethoate, deltamethrin, triazolone and carbendazim were supplied by Chongqing Entry Exit Inspection and Quarantine Bureau. All other chemicals used were of analytical grade. All aqueous solutions were prepared with deionized (DI) water generated from a Millipore Direct-Q Water system.

Aptamer was adopted from the work of others [31]. All synthetic oligonucleotides were provided by Sangon Inc. (Shanghai, China). All oligonucleotide stock solutions were prepared with 15 mM phosphate-buffered saline (PBS, pH 7.4) and stored at 4 °C. The base sequences of synthetic oligonucleotides were as follows:

Aptamer probe: 5′-CCTGCCACGCTCCGCAAGCTTAGGGTTACG CCTGCAGCGATTCTTGATCGCGCTGCTGGTAATCCTTCTTTAAGCTTGG CACCCGCATCGT-3′.

Amino-modified capture probe (AMP): 5′-NH_2-$(CH_2)_6$-ACGATGCGGGTGCCAAGCTT-3′.

2.2. Characterization

Scanning electron microscopy (SEM) images were collected on FEI Nova 400 FEG-Sem (FEI, USA) at an acceleration voltage of 15.0 kV. Fourier transform infrared spectroscopy (FT-IR) was measured on a Bruker-Tensor 27IR spectrophotometer. Cyclic voltammetric (CV) and differential pulse voltammetry (DPV) were performed on a CHI 660E electrochemistry workstation (CHI Instruments of Shanghai, China). A conventional three-electrode system was employed with a glassy carbon electrode (GCE), a silver/silver chloride (Ag/AgCl) reference electrode and a platinum wire counter electrode as the working, reference and counter electrode, respectively.

2.3. Fabrication of CuO NFs-SWCNTs-modified GCE

The CuO NFs were prepared according to the previous literature [32]. In short, $CuSO_4{\cdot}5H_2O$ was dissolved with water in a beaker under continuous stirring at 80 °C for 2 min. NaOH solution was added dropwise to the above $CuSO_4$ solution, and the black precipitates were formed. After being continuously stirred for 20 min, the precipitates were naturally cooled at room temperature. Then, the precipitates were centrifuged four times at 10,000 rpm for 2 min in water and anhydrous ethanol, respectively. Finally, the black product (CuO NFs) was dried in a vacuum oven. CuO NFs were suspended at 3 mg/mL in ethanol for further use.

The c-SWCNTs were homogenously dispersed in DMF under sonication to obtain a 1 mg/mL suspension. Prior to electrode modification, the 3-mm diameter bare GCE was polished by 0.3 μm and 0.05 μm aluminum slurries sequentially, sonicated in deionized water for 5 min, and dried by nitrogen. Firstly, 5 μL Nafion solution (0.05 wt%) was dropped onto the surface of GCE and allowed to dry at room temperature. The as-prepared electrode was denoted as Nafion/GCE. Next, 10 μL mixture with an appropriate volume ratio of CuO NFs suspension and c-SWCNTs suspension was loaded on the Nafion/GCE. The electrode was denoted as CuO NFs-SWCNTs/Nafion/GCE.

2.4. Immobilization of amino-modified capture probe and hybridization of aptamer on CuO NFs-SWCNTs-modified GCE

The CuO NFs-SWCNTs/Nafion/GCE was incubated with a freshly prepared solution (10.0 mM EDC, 16.0 mM NHS) for 30 min to activate the carboxylic groups of c-SWCNTs. Then the electrode was immersed in a solution containing 20 nM AMP in 15 mM PBS (pH 7.0) for 2 h. AMP was immobilized on the surface of CuO NWs-SWCNTs/Nafion/GCE by covalent amide bonds forming between the 5′-amino group of AMP and the carboxyl group of c-SWCNTs. Subsequently, the modified electrode was rinsed with 15 mM, pH 7.0 PBS to remove unbound AMP, and incubated with 20 nM aptamer for 1 h to form the hybridization between AMP and aptamer. Finally, the as-prepared electrode was washed with PBS to remove unbound aptamer, and denoted as Aptamer/AMP/CuO NFs-SWCNTs/Nafion/GCE. Besides, control electrodes (including bare GCE, Nafion/GCE, SWCNTs/Nafion/GCE, CuO NFs-SWCNTs/Nafion/GCE and AMP/CuO NFs-SWCNTs/Nafion/GCE) were fabricated to reveal the effect of individual component in sensing.

2.5. Electrochemical measurements of chlorphrifos

The as-prepared electrode was incubated with 45 μM MB solution for 30 min, resulting in the accumulation of MB onto the aptamer-modified GCE surface. Next, the electrode was washed with PBS thoroughly. After incubation with different concentrations of chlorphrifos, the electrode was detected by DPV to measure the decrease of MB accumulation in 15 mM, pH 7.0 PBS solution.

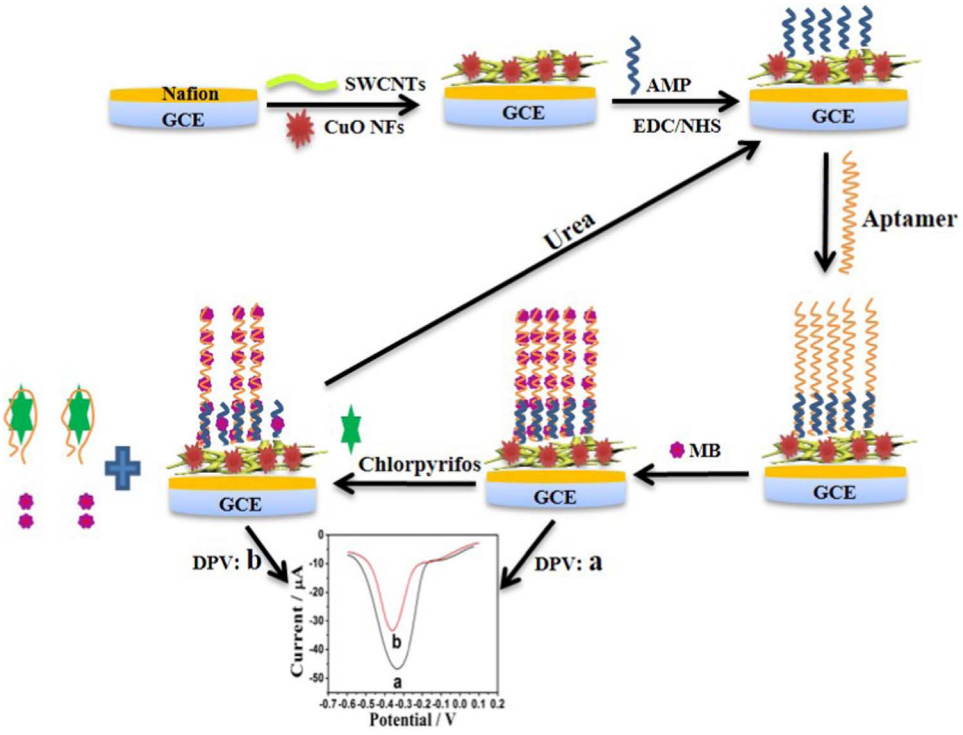

Scheme 1. Schematic illustration of the regenerative electrochemical aptasensor for selective detection of chlorpyrifos.

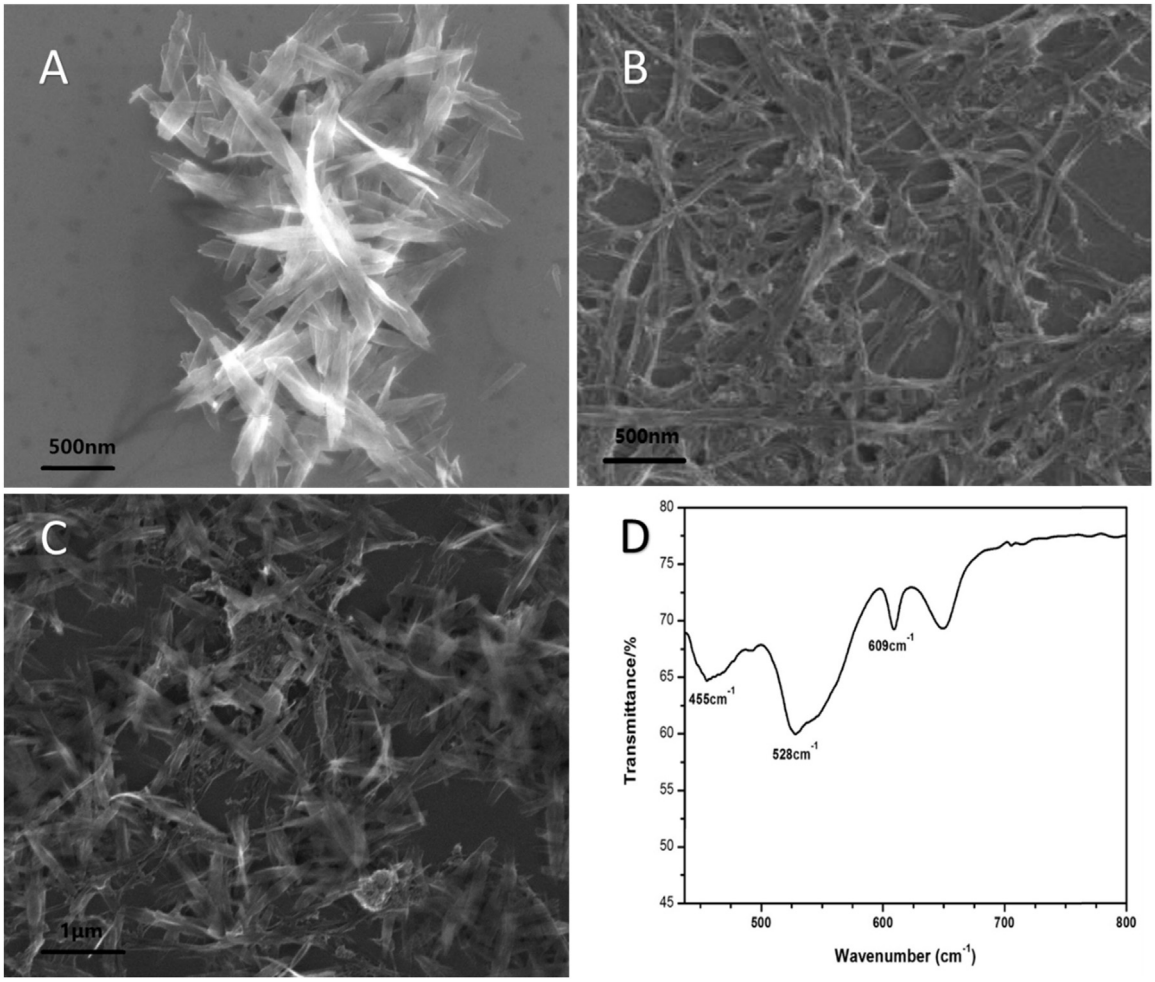

Fig. 1. SEM images of CuO NFs (A), SWCNTs (B), and CuO NFs-SWCNTs hybrid composite (C), respectively. (D) FT-IR spectra of CuO NFs.

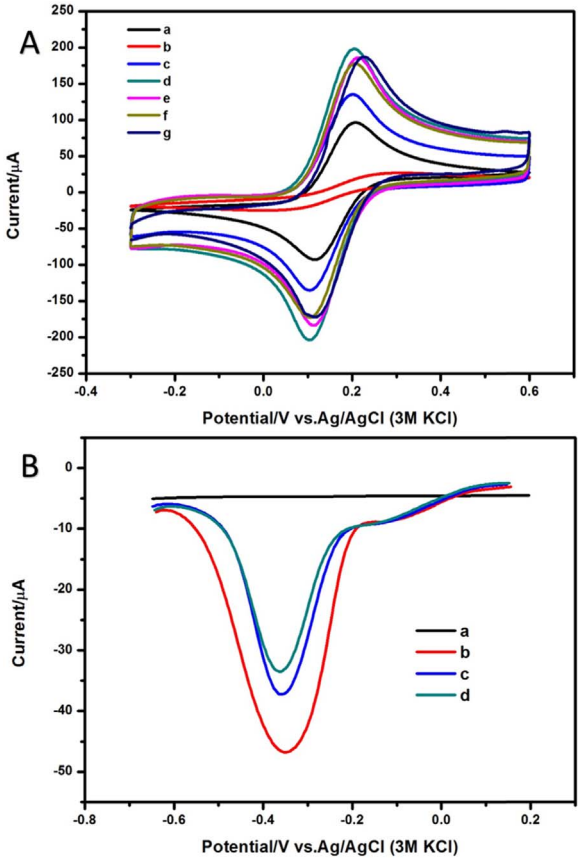

Fig. 2. (A) CVs of 5.0 mM $[Fe(CN)_6]^{3-/4-}$ and 0.1 M KCl solution at different modified electrodes: (a) bare GCE; (b) Nafion/GCE; (c) SWCNTs/Nafion/GCE; (d) CuO NFs-SWCNTs/Nafion/GCE; (e) AMP/CuO NFs-SWCNTs/Nafion/GCE; (f) Aptamer/AMP/CuO NFs-SWCNTs/Nafion/GCE; (g) Regeneration after the detection of chlorpyrifos; (B) DPVs of Aptamer/AMP/CuO NFs-SWCNTs/Nafion/GCE after incubating in different solutions: (a) 15 mM PBS, pH 7.0; (b) 50 μM MB; (c) 50 μM MB_5 ng/mL chlorpyrifos; (d) 50 μM MB_100 ng/mL chlorpyrifos.

To study the feasibility of the proposed sensor, the detections of chlopyrifos spiked in apples and celery cabbages were performed. Apples and celery cabbages were purchased from the supermarket in Chongqing. Firstly, the samples were homogenized to pulp in a mortar with the PBS buffer solution and centrifuged for 20 min at 7000 rpm to remove the solids. Then the supernatant was filtered to remove large particles through a 0.22 μm filter. Finally, the spiked real samples with three different concentrations of chlopyrifos were examined through DPV detection.

3. Results and discussion

3.1. Sensing principle of the as-prepared aptasensor

The schematic diagram of the sensing mechanism is shown in Scheme 1. Nafion, used as an adhesive agent [33], was loaded on the bare GCE. Then the electrode was coated with a nanocomposite consisting of CuO NFs and c-SWCNTs. The synergistic effect of CuO NFs-SWCNTs nanocomposite can expand the surface area of the electrode and enhance the electron transfer, while c-SWCNTs were responsible for enhancing the ability of immobilizing the aminated probes and hybridization between aptamers and aminated probes.

AMP was complementary to a part of 3′ distal sequence of aptamer and was labeled with an amino group at its 5′ distal terminus. AMP was immobilized on c-SWCNTs via covalent bonding between the carboxyl group on c-SWCNTs and its amino group. Aptamer, which specifically recognized chlorpyrifos, was then partly hybridized with capture probe on the electrode surface [34]. In this work, DPV of MB was applied to monitor the hybridization event. MB, a redox indicator for DNA hybridization, can bind with nucleic acid chains (single-stranded DNA or double-stranded DNA) in a non-covalent manner [35,36]. The major reactions of the MB with nucleic acid chain are the specific recognition of MB with unbound guanine base [37], the intercalation into double-stranded DNA base pairs and the electrostatic adsorption [38,39]. After the addition of chlorpyrifos, the formation of more compact aptamer-chlorpyrifos complex structure resulted in the decrease amount of MB bound to guanine bases in the aptamer domain. Consequently, aptamer was forced to dissociate from semi-duplex, resulting in the fleeing of MB from the sensing interface. Thus, the DPV peak current of MB decreased with the increase of chlorpyrifos concentration and the change of DPV signal before (curve a) and after (curve b) the addition of chlorpyrifos can be used to quantify chlorpyrifos. However, the binding or the fleeing of MB was a tedious process, which indicated that the proposed sensor was not suitable for rapid detection. It is well known that urea can denature nucleic acids by stronger interaction of hydrogen bond with nucleic acid bases. This aptasensor can be easily regenerated by immersing in urea solution and furthermore be recombined with the aptamer. Hence, the biosensor can achieve repeated detection of chlorpyrifos.

3.2. Characterization of CuO NFs-SWCNTs hybrid composite

A SEM image of the as-prepared CuO NFs is shown in Fig. 1A. Hierarchical CuO NFs presented a flower-like architecture and consisted of many nanoplate building blocks. These blocks were connected together and arranged disorderly to form a three-dimensional morphology with a strong contrast between the front-edge (white) and the back-edge (gray). Fig. 1D shows the FT-IR spectra of CuO NFs, whose peaks at 455 cm^{-1}, 528 cm^{-1} and 609 cm^{-1} could be attributed to the Cu-O bond stretching vibration [40,41]. As is shown in Fig. 1B, the crude SWCNTs were obviously rough and had a network structure, indicating that they were very flexible and had a large surface area. Fig. 1C is a typical SEM image of CuO NFs-SWCNTs hybrid composite. It could be seen that the nanocomposite was successfully prepared by the intertwining of SWCNTs on CuO NFs.

3.3. Electrochemical characterization of the different modified electrodes

As shown in Fig. 2A, different preparation stages of the biosensor were studied to evaluate and characterize the fixation effect by CV in 5.0 mM $[Fe(CN)_6]^{3-/4-}$ and 0.1 M KCl. Firstly, the CV of bare electrode (curve a) was measured and it demonstrated the defined reversible redox behavior of $[Fe(CN)_6]^{3-/4-}$. The addition of nafion to the bare electrode reduced the CV current of the modified electrode (curve b), indicating that negatively charged nafion significantly hindered the electron transfer rate between the electrode and $[Fe(CN)_6]^{3-/4-}$. Then, SWCNTs were fixed on the surface of Nafion/GCE (curve c), and consequently there was a sharp increase in CV, which may be due to the good conducting performance of SWCNTs. The CV peak current of CuO NFs-SWCNTs/Nafion/GCE (curve d) was further increased and reached the highest peak, which could be attributed to the fact that the stereochemical structure of CuO NFs-SWCNTs nanocomposite greatly increased the number of reaction sites on SWCNTs and synergistically promoted electron transfer. Subsequently, the CV of the AMP/CuO NFs-SWCNTs/Nafion/GCE (curve e) decreased slightly. The peak current of CV (curve f) was reduced further after the hybridization of aptamer on the biosensor because both the negatively charged nucleic acid probe and aptamer had an electrostatic repulsion to anionic $[Fe(CN)_6]^{3-/4}$ [42]. Finally, after the regeneration of the above electrode in urea, CV (curve g) was almost flat from AMP/CuO NFs-SWCNTs/Nafion/GCE, indicating that the denaturation of urea could break residual semi-duplex, resulting in the dissociation of the aptamer from the sensing surface. Fig. 2B depicts DPV behaviors of Aptamer/AMP/CuO NFs-SWCNTs/Nafion/GCE after incubating in different solutions. The peak current near −0.35 V was assigned to the MB and its intensity decreased with the increase of chlorpyrifos concentration, suggesting that the formation of aptamer-chlorpyrifos complex results in the fleeing of MB from the sensing interface.

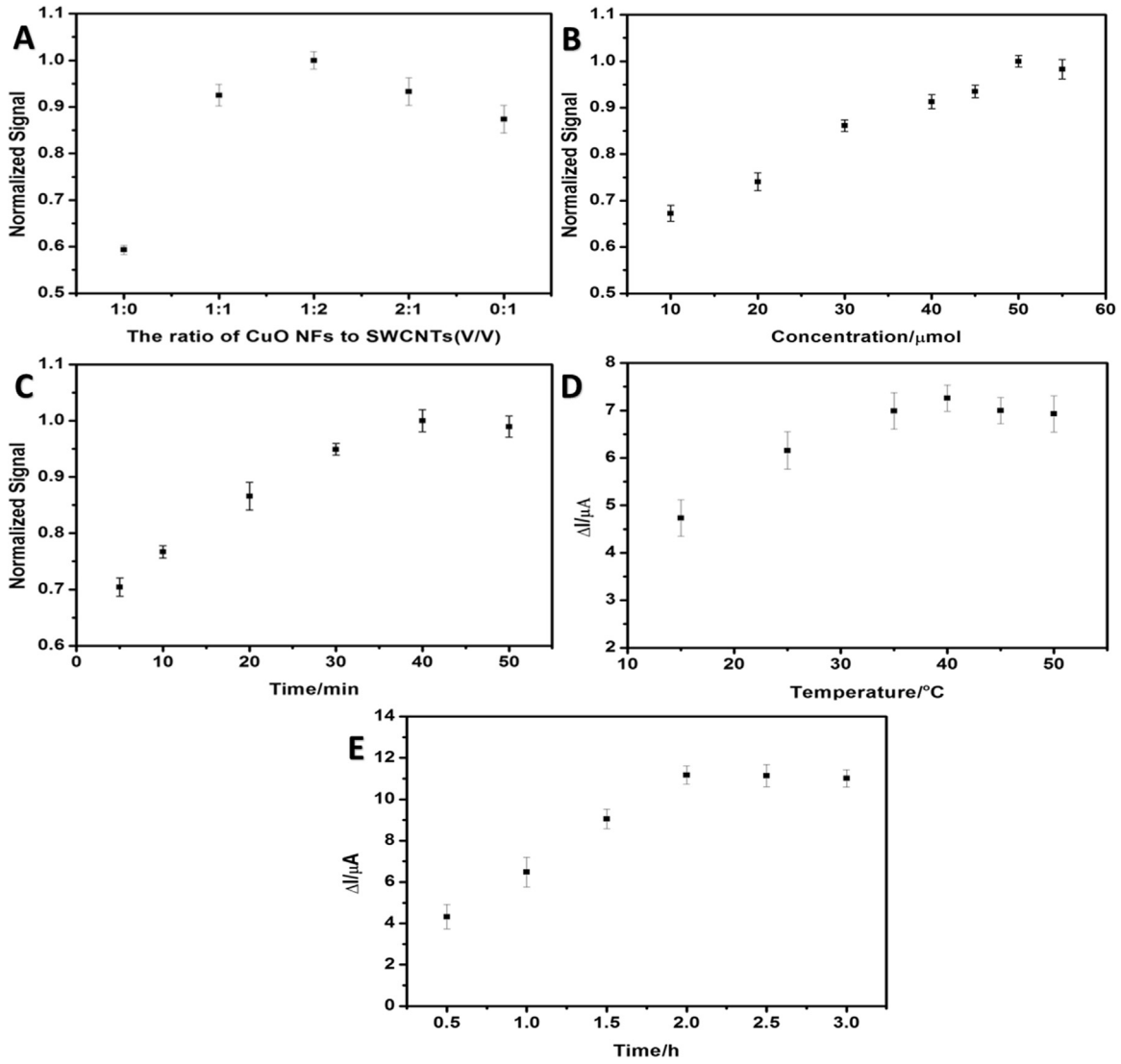

Fig. 3. Optimization of assay conditions: (A) the ratio of CuO NFs to SWCNTs, (B) MB incubation concentration on Aptamer/AMP/CuO NFs-SWCNTs/Nafion/GCE, (C) MB incubation time on Aptamer/AMP/CuO NFs-SWCNTs/Nafion/GCE hybridization temperature, (D) Chlorpyrifos incubation temperature, (E) Chlorpyrifos incubation time.

3.4. Optimization of experimental conditions

To optimize assay conditions of the biosensor, DPV was used to optimize these parameters, including the ratio of CuO NFs to SWCNTs, MB incubation concentration, MB incubation time, chlorpyrifos incubation temperature and chlorpyrifos incubation time. In order to obtain the optimal value of one parameter, all other parameters were implemented under their optimum conditions. Because the proportion of different materials would greatly affect the performance of biosensors, the ratio of CuO NFs to SWCNTs was firstly optimized. As shown in Fig. 3A, the ratio of CuO NFs (3 mg/mL) to SWCNTs (1 mg/mL) at 1:2 achieved the highest normalized signal with a loading volume of 10 μL.

To obtain excellent analytical performance, the concentration and incubation time of MB were investigated. As illustrated in Fig. 3B, the signal increases with the increase of the MB concentration. However, when the MB concentration reached 50 μM, continuous increase of MB concentration did not significantly lead to an increase of the signal. The response increased significantly from 0 to 40 min (Fig. 3C), and reached a plateaus after 40 min, indicating that a saturation had been obtained. Thus, the concentration and incubation time of MB were optimized at 50 μM and 40 min in the following experiments respectively.

The effects of chlorpyrifos incubation temperature and incubation time were also investigated. As shown in Fig. 3D, the current response is detected from 15 to 50 ˚C and reaches the top at 40 ˚C. It can be seen from Fig. 3E that the current response increases gradually from 0 to 2 h and remains stable thereafter, indicating that the specific binding interaction between aptamers and chlorpyrifos reaches saturation. Therefore, 40 ˚C and 2 h were set as the optimal chlorpyrifos incubation temperature and time respectively.

3.5. Sensitivity for chlorphrifos detection

Under the optimal operating conditions, the sensitivity of the biosensor was investigated after incubation with different concentrations of chlorpyrifos. As shown in Fig. 4A, the peak current of DPV decreased gradually with increasing chlorpyrifos concentration. This is due to the fact that the dissociation of semi-duplex caused by the formation of complex between chlorpyrifos and aptamer was accompanied by the reduction of MB from the surface of electrode. As shown in Fig. 4B and Table S1, the linear equation between ΔI and log C was $\Delta I = 4.028 \log C + 5.589$ ($R = 0.993$) from 0.1 to 150 ng/mL for chlorpyrifos, in which ΔI represented the D value of peak current between 0 ng/mL and the one in the presence of chlorpyrifos, log C represented the logarithm of chlorphrifos concentration. The calculated limit of detection (LOD) for chlorpyrifos was 70 pg/mL ($S/N = 3$), which was better than other aptamer-based chlorpyrifos biosensor (0.33 ng/mL) [29]. The excellent

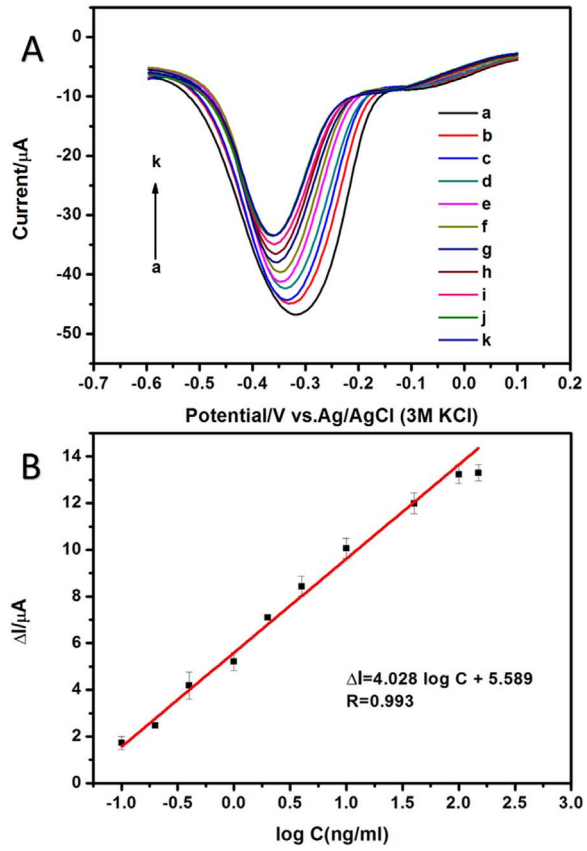

Fig. 4. (A) DPVs on the Aptamer/AMP/CuO NFs-SWCNTs/Nafion/GCE in 15 mM, pH 7.0, PBS containing different concentrations of chlorphrifos (curves a–k: 0, 0.1, 0.2, 0.4, 1, 2, 4, 10, 40, 100 and 150 ng/mL, respectively); (B) linear calibration curve of peak current changes of MB (ΔI) versus the log of chlorphrifos concentrations (log C). Error bars show the standard deviations of measurements taken from three independent experiments.

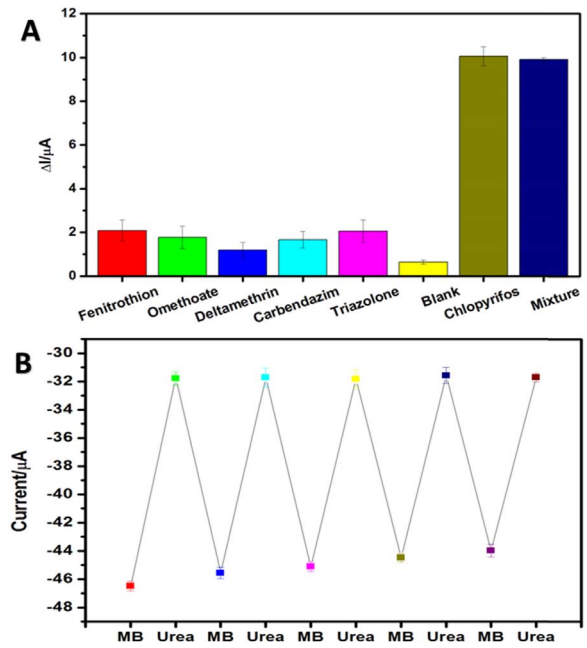

Fig. 5. (A) Selectivity evaluation of the aptasensor detection of fenitrothion, omethoate, deltamethrin, carbendazim, triazolone, blank, chlorpyrifos and the mixture consisting of the above interference and chlorpyrifos; (B) Reversible changes of MB peak currents for the biosensor immersed alternately in the solution of 20 nM aptamer, 50 μM MB, and 8 M urea. Error bar represents the standard deviation of three replicate detections from one electrode.

sensing performance of this aptasensor could be attributed to two reasons: one was the 3D morphology structure of CuO NFs, which provided a large surface-to-volume ratio; the other was the synergistic effect of excellent conducting performance of SWCNTs and CuO NFs.

3.6. Selectivity, repeatability and regeneration of the biosensor

To assess the selectivity of the as-prepared biosensor, other interferential pesticides that may coexist with chlorpyrifos were selected for evaluation. Fig. 5. A shows the DPV signals of interferent components, chlorpyrifos, and their mixture. The concentrations of interferent components containing fenitrothion, omethoate, deltamethrin, carbendazim and triazolone were kept at 50 ng/mL, and chlorpyrifos was kept at 10 ng/mL, while blank was the PBS solution of 15 mM, pH 7.0. As we can see, chlorpyrifos and the mixture were distinctly discriminated from other objects under the same experimental conditions. Moreover, in order to assess the sample matrix effect, we also did interference test in the cabbage samples by the same method (Fig. S1). The response of the biosensor was clearly observable for chlorpyrifos whereas the biosensor rarely responded to interferents. This can be ascribed to the high specificity of chlorpyrifos aptamer, indicating that the as-prepared biosensor had high selectivity for chlorpyrifos detection and good interference resistance, while the sample matrix had hardly any effect on the selectivity study. The repeatability of the aptasensor was evaluated by analyzing 10 ng/mL chlorpyrifos solution with five electrodes. The relative standard deviation (RSD) of the measurements for the five electrodes was 4.23%, suggesting the acceptable repeatability of the proposed aptasensor.

Reusability is also an important factor of a sensor in the practical application. However, to our knowledge, few studies have investigated the regeneration of chlorpyrifos aptasensor. In this work, urea was employed to remove semi-duplex from the sensing electrode. After the incubation with MB, the biosensor was regenerated by immersing in urea solution for 0.5 h at room temperature, and the regenerated electrode could be re-used. Fig. 5B shows the DPV peak current of the biosensor immersed alternately in the solutions of 20 nM aptamer, 50 μM MB, and 8 M urea for five regeneration cycles. It can be seen that the peak current changed reversibly, which could be attributed to the insertion and release of MB at the chains of nucleic acids. After five regeneration cycles, there was a slight decrease in signal compared with its initial current, suggesting that the biosensor can be easily regenerated. However, the peak current did not restore to Fig. 2B (a), probably due to the non-specific adsorption of MB onto the electrode surface. As summarized in Table S2, the proposed biosensor showed good analytical performances and especially had the capacity of regeneration in chlopyrifos aptasensor.

3.7. Analysis of real samples

To further evaluate the potential of the proposed sensor in practical application, the detections of chlopyrifos spiked in apples and celery cabbages were performed respectively. The solutions of extraction samples were added with chlopyrifos standard solution at three different concentrations (1.0, 10.0, 50.0 ng/mL). Table 1 shows the results of recovery testing ranging from 95.58 ± 4.32% to 106.72 ± 2.66%, indicating the excellent reliability of the developed biosensor for the detection of chlopyrifos in real samples.

4. Conclusions

In summary, a sensitive, selective and regenerative electrochemical aptasensor was developed for detection of chlopyrifos based on CuO NFs-SWCNTs nanocomposite. Under the optimized conditions, the proposed chlopyrifos aptasensor exhibited high sensitivity, good reproducibility, excellent selectivity, and low limit of detection. Such excellent sensing performance may be attributed to large surface-to-

Table 1
Recovery studies of spiked chlopyrifos in apples and celery cabbages (each result was the average of three determinations).

Sample	Spiked (ng/mL)	Found (ng/mL)	RSD (%)	Recovery (%)
Apple	1.0	0.97	2.52	97.08
	10.0	10.66	2.66	106.72
	50.0	51.43	4.82	102.85
Celery cabbage	1.0	0.95	2.25	97.07
	10.0	10.30	4.62	103.05
	50.0	47.99	4.32	95.98

volume ratio by CuO NFs and the synergistic effect of electrical conductivity from CuO NFs and SWCNTs. The sensor was successfully applied in the detection of chlopyrifos in the real samples, and obtained satisfactory recoveries. In addition, the biosensor can be easily regenerated by urea for continued use. All these features indicate that the developed nanocomposite based strategy is a promising way to improve the performances and promote recycling of aptasensor.

Acknowledgements

This work was supported by the National Natural Science Foundation of China (No. 31171684 and 31101284), Chongqing Science and Technology Commission (CSTC2015shmszxl20097), Chongqing Graduate Student Research Innovation Project (No. CYB16038), the Workstation in Sichuan Province GY2015-01 and sharing fund of Chongqing university's large equipment.

Appendix A. Supplementary material

Supplementary data associated with this article can be found in the online version at http://dx.doi.org/10.1016/j.talanta.2017.08.086.

References

[1] J.E. Casida, K.A. Durkin, Anticholinesterase insecticide retrospective, Chem. Biol. Interact. 203 (2013) 221–225.
[2] W.N. Aldridge, E. Reiner, Enzyme Inhibitors as Substrates: Interactions of Esterases with Esters of Organophosphorus and Carbamic Acids, North-Holland Publishing Company, Amsterdam, 1972.
[3] J. Bajgar, Organophosphates/nerve agent poisoning: mechanism of action, diagnosis, prophylaxis, and treatment, Adv. Clin. Chem. 38 (2004) 151–216.
[4] T.T. Marrs, R.L. Maynard, F. Sidell, Chemical Warfare Agents: Toxicology and Treatment, John Wiley & Sons, 2007.
[5] K.A. Lewis, J. Tzilivakis, D.J. Warner, A. Green, An international database for pesticide risk assessments and management, Hum. Ecol. Risk Assess. 22 (2016) 1050–1064.
[6] D.C. Smegal, Human Health Risk Assessment Chlorpyrifos, US Environmental Protection Agency, Office of Prevention, Pesticides and Toxic Substances, Office of Pesticide Programs, Health Effects Division, US Government Printing Office, Washington, DC, 2000, pp. 1–131.
[7] C.P. Karunanayake, J.J. Spinelli, J.R. McLaughlin, J.A. Dosman, P. Pahwa, H.H. McDuffie, Hodgkin lymphoma and pesticides exposure in men: a Canadian case-control study, J. Agromed. 17 (2012) 30–39.
[8] G.J. Oostingh, G. Wichmann, M. Schmittner, I. Lehmann, A. Duschl, The cytotoxic effects of the organophosphates chlorpyrifos and diazinon differ from their immunomodulating effects, J. Immunotoxicol. 6 (2009) 136–145.
[9] P. Duramad, I.B. Tager, J. Leikauf, B. Eskenazi, N.T. Holland, Expression of Th1/Th2 cytokines in human blood after in vitro treatment with chlorpyrifos, and its metabolites, in combination with endotoxin LPS and allergen der p1, J. Appl. Toxicol. 26 (2006) 458–465.
[10] N. Guiñazú, V. Rena, S. Genti-Raimondi, V. Rivero, G. Magnarelli, Effects of the organophosphate insecticides phosmet and chlorpyrifos on trophoblast JEG-3 cell death, proliferation and inflammatory molecule production, Toxicol. Vitr. 26 (2012) 406–413.
[11] L.J. He, X.L. Luo, H.X. Xie, C.J. Wang, X.M. Jiang, K. Lu, Ionic liquid-based dispersive liquid-liquid microextraction followed high-performance liquid chromatography for the determination of organophosphorus pesticides in water sample, Anal. Chim. Acta 655 (2009) 52–59.
[12] S. Rai, A.K. Singh, A. Srivastava, S. Yadav, M.H. Siddiqui, M.K.R. Mudiam, Comparative evaluation of QuEChERS method coupled to DLLME extraction for the analysis of multiresidue pesticides in vegetables and fruits by gas chromatography-mass spectrometry, Food Anal. Method. 9 (2016) 2656–2669.
[13] G. Jeanty, C. Ghommidh, J. Marty, Automated detection of chlorpyrifos and its metabolites by a continuous flow system-based enzyme sensor, Anal. Chim. Acta 436 (2001) 119–128.
[14] X.T. Li, D.Z. Zhu, Z.H. Ma, L.G. Pan, D. Wang, J.H. Wang, Feasibility study of the detection of chlorpyrifos residuals on apple skin based on infrared micro-imaging, Opt. Eng. 51 (2012) 8.
[15] H. Li, J. Li, Q. Xu, X. Hu, Poly (3-hexylthiophene)/TiO2 nanoparticle-functionalized electrodes for visible light and low potential photoelectrochemical sensing of organophosphorus pesticide chlopyrifos, Anal. Chem. 83 (2011) 9681–9686.
[16] S. Li, W. Liang, F. Zheng, X. Lin, J. Cai, Ascorbic acid surface modified TiO 2-thin layers as a fully integrated analysis system for visual simultaneous detection of organophosphorus pesticides, Nanoscale 6 (2014) 14254–14261.
[17] G.L. Qian, L.M. Wang, Y.R. Wu, Q. Zhang, Q. Sun, Y. Liu, F.Q. Liu, A monoclonal antibody-based sensitive enzyme-linked immunosorbent assay (ELISA) for the analysis of the organophosphorous pesticides chlorpyrifos-methyl in real samples, Food Chem. 117 (2009) 364–370.
[18] J. Li, M. Sun, X. Wei, L. Zhang, Y. Zhang, An electrochemical aptamer biosensor based on "gate-controlled" effect using beta-cyclodextrin for ultra-sensitive detection of trace mercury, Biosens. Bioelectron. 74 (2015) 423–426.
[19] Z.S. Qian, X.Y. Shan, L.J. Chai, J.R. Chen, H. Feng, A fluorescent nanosensor based on graphene quantum dots-aptamer probe and graphene oxide platform for detection of lead (II) ion, Biosens. Bioelectron. 68 (2015) 225–231.
[20] G. Liang, Y. Man, X. Jin, L. Pan, X. Liu, Aptamer-based biosensor for label-free detection of ethanolamine by electrochemical impedance spectroscopy, Anal. Chim. Acta 936 (2016) 222–228.
[21] X. Miao, Z. Li, A. Zhu, Z. Feng, J. Tian, X. Peng, Ultrasensitive electrochemical detection of protein tyrosine kinase-7 by gold nanoparticles and methylene blue assisted signal amplification, Biosens. Bioelectron. 83 (2016) 39–44.
[22] Y.T. Tseng, C.H. Wang, C.P. Chang, G.B. Lee, Integrated microfluidic system for rapid detection of influenza H1N1 virus using a sandwich-based aptamer assay, Biosens. Bioelectron. 82 (2016) 105–111.
[23] R. Bala, M. Kumar, K. Bansal, R.K. Sharma, N. Wangoo, Ultrasensitive aptamer biosensor for malathion detection based on cationic polymer and gold nanoparticles, Biosens. Bioelectron. 85 (2016) 445–449.
[24] F. Barahona, C.L. Bardliving, A. Phifer, J.G. Bruno, C.A. Batt, An aptasensor based on polymer-gold nanoparticle composite microspheres for the detection of malathion using surface-enhanced Raman spectroscopy, Ind. Biotechnol. 9 (2013) 42–50.
[25] A.I. Ayesh, Z. Karam, F. Awwad, M.A. Meetani, Conductometric graphene sensors decorated with nanoclusters for selective detection of Hg2+ traces in water, Sens. Actuators B Chem. 221 (2015) 201–206.
[26] J. Lavanya, N. Gomathi, High-sensitivity ascorbic acid sensor using graphene sheet/graphene nanoribbon hybrid material as an enhanced electrochemical sensing platform, Talanta 144 (2015) 655–661.
[27] J. Turan, M. Kesik, S. Soylemez, S. Goker, S. Coskun, H.E. Unalan, L. Toppare, An effective surface design based on a conjugated polymer and silver nanowires for the detection of paraoxon in tap water and milk, Sens. Actuators B Chem. 228 (2016) 278–286.
[28] R.N. Ma, J.J. Hu, Z.W. Cai, H.X. Ju, Highly selective enrichment of phosphopeptides with high-index facets exposed octahedral tin dioxide nanoparticles for mass spectrometric analysis, Talanta 119 (2014) 452–457.
[29] Y. Jiao, H. Jia, Y. Guo, H. Zhang, Z. Wang, X. Sun, J. Zhao, An ultrasensitive aptasensor for chlorpyrifos based on ordered mesoporous carbon/ferrocene hybrid multiwalled carbon nanotubes, RSC Adv. 6 (2016) 58541–58548.
[30] Y. Jiao, W. Hou, J. Fu, Y. Guo, X. Sun, X. Wang, J. Zhao, A nanostructured electrochemical aptasensor for highly sensitive detection of chlorpyrifos, Sens. Actuators B Chem. 243 (2017) 1164–1170.
[31] Z.J. lei, C.Z. Zhang, Y. Liu, L. Wang, Selection of chlorpyrifos-binding ssDNA aptamer by SELEX, Jiangsu J. Agr. Sci. 28 (2012) 198–203.
[32] S. Sun, Y. Sun, X. Zhang, H. Zhang, X. Song, Z. Yang, A surfactant-free strategy for controllable growth of hierarchical copper oxide nanostructures, CrystEngComm 15 (2013) 5275.
[33] M.S. McGovern, E.C. Garnett, C. Rice, R.I. Masel, A. Wieckowski, Effects of Nafion as a binding agent for unsupported nanoparticle catalysts, J. Power Sources 115 (2003) 35–39.
[34] Y. Dai, B. Chakraborty, B. Ge, H.Z. Yu, Adenosine-triggered elimination of methylene blue noncovalently bound to immobilized functional dsDNA-aptamer constructs, J. Phys. Chem. B 116 (2012) 6361–6368.
[35] A.A. Gorodetsky, M.C. Buzzeo, J.K. Barton, DNA-mediated electrochemistry, Bioconjugate Chem. 19 (2008) 2285–2296.
[36] S.O. Kelley, N.M. Jackson, M.G. Hill, J.K. Barton, Long-range electron transfer through DNA films, Angew. Chem. Int. Ed. 38 (1999) 941–945.
[37] A. Erdem, K. Kerman, B. Meric, M. Ozsoz, Methylene blue as a novel electrochemical hybridization indicator, Electroanalysis 13 (2001) 219–223.
[38] A. Tani, A.J. Thomson, J.N. Butt, Methylene blue as an electrochemical discriminator of single- and double-stranded oligonucleotides immobilised on gold substrates, Analyst 126 (2001) 1756–1759.
[39] M. Castano-Alvarez, M. Fernandez-Abedul, A. Costa-Garcia, Electroactive intercalators for DNA analysis on microchip electrophoresis, Electrophoresis 28 (2007) 4679–4689.
[40] İ.Y. Erdoğan, Ö. Güllü, Optical and structural properties of CuO nanofilm: its diode application, J. Alloy. Compd. 492 (2010) 378–383.
[41] M.R. Johan, M.S.M. Suan, N.L. Hawari, H.A. Ching, Annealing effects on the properties of copper oxide thin films prepared by chemical deposition, Int. J. Electrochem. Sci. 6 (2011) 6094–6104.
[42] Z. Lin, L. Chen, G. Zhang, Q. Liu, B. Qiu, Z. Cai, G. Chen, Label-free aptamer-based electrochemical impedance biosensor for 17beta-estradiol, Analyst 137 (2012) 819–822.